JOURNAL OF MATERIALS SCIENCE 31 (1996) 5443–5449

Spot welding of metal laminated composites

H. ENGSTROEN
The Royal Institute of Technology, Department of Materials Technology, 10044 Stockholm, Sweden

J. DURÁN, J. M. AMO, A. J. VÁZQUEZ
Centro Nacional de Investigaciones Metalúrgicas, Av. Gregorio del Amo/ 8, 28040-Madrid, Spain

Composite materials of steel sheets joined by interlayers of zinc or lead–tin, show very good impact and corrosion resistance properties. Resistance spot-weld characteristics of these composite materials made of steel sheets and non-ferrous metals have been tested. Spot welds of composites with both zinc and lead–tin interlayers present good behaviour in peeling tests. Shear tests of the welds also show very high strength, probably as a consequence of simultaneous brazing because of the alloyed layer of non-ferrous material around the weld spot. This good welding behaviour enhances the possibilities of application of this composite.

1. Introduction

A large number of studies concerning metal matrix composites have been published during the last 20 years. The main interest has been concentrated in characterizing and developing materials based on reinforcement used in the form of fibres, whiskers and particles. The benefit of composite materials made of layers is also clear. Mats of wire composites are piled at different angles, typically 30°, 60° and 90°, to obtain a more isotropic material.

The direct use of sheets in place of the mats presents another opportunity to fabricate sheet composite materials. Nevertheless, far less interest has been directed to the more isotropic materials made of metal laminate composites.

The possibility of using layers of different metals in industrial practice has mainly been utilized as claddings or in sandwich structures. Several studies have shown that if structures with a larger number of metal layers are produced, improved properties, compared with single sheet materials, can be obtained. Embury *et al.* [1] studied the impact properties of brazed and explosively bonded low-carbon steel laminates [1]. Stuart and Crouch [2] highlighted the possibility of using adhesively bonded aluminium laminates to improve perforation characteristics, while Sherby and co-workers demonstrated the benefits of ultrahigh carbon steel-based laminate composites [3–6].

The possibility of producing multilaminar metal composites using a relatively inexpensive manufacturing hot-dipping process has been reported by Vázquez–Vaamonde and de Damborenea [7]. Several separated steel sheets are introduced simultaneously into a non-ferrous molten metal bath at temperatures below the steel melt temperature. As the sheets were withdrawn from the bath, a pressure is applied. The still liquid metal on the surface of the sheets is trapped between them when pressed and solidifies, forming interlayers of non-ferrous metal between the steel sheets. In addition to the enhancement of impact resistance properties of this multilaminar structure, if the molten metal is properly chosen, some inherent corrosion resistance can be obtained.

The main benefit of the multilaminar structure of this material is its impact resistance perpendicular to the sheet surface. Very good mechanical properties have been reported [8–10] and the intrinsic corrosion resistance properties of the composite due to the zinc or lead–tin interlayer has been well discussed. Nevertheless, the development of possible applications of this composite lies in the joining properties of the material. In this paper results of a preliminary research about the resistance spot-welding characteristics of two kinds of multilaminar composites produced with this hot-dipping process, are presented.

2. Experimental procedure

2.1. Preparation of composites

Multilaminar composites containing three 0.5 mm thick steel sheets were produced with the process described above. The sheet dimensions were 175 mm × 100 mm. The steel composition was 0.07 C, 0.04 Si, 0.20 Mn, 0.013 P, 0.009 S and 0.069 Al(wt%).

Two different molten baths were used as matrix: (i) pure zinc, zinc 99.99%, iron-saturated bath with 0.01% Al additions, and (ii) 95% Pb–5% Sn. The use of the zinc bath produces several intermetallic layers in the interlayer between the steel reinforcing sheets according to the Zn–Fe equilibrium diagram. On the contrary, the lead bath, with a small tin percentage,

0022–2461

produces almost no intermetallic layers in the interlayer between the steel reinforcing sheets.

The steel sheets were immersed in a metal bath at a temperature of 450° C for 2–6 min. Examples of the microstructures produced are shown in Fig. 1. As can be seen, the matrix thicknesses, i.e. the layers of matrix between the steel sheets, varied but were always between one-third and one-tenth of the thickness of the steel sheets according to the dipping time and the pressure applied. The steel has a ferrite microstructure. In the zinc interlayers, a significant amount of intermetallic ZnFe is seen. The lead–tin interlayers consist of pure lead.

2.2. Mechanical properties

The mechanical properties of the steel as measured in a tensile test are presented in Table I.

The adherence between sheets in this multilaminar composite does not influence the free through-thickness deformation of the component sheets. This is illustrated in Fig. 2a and b, where the independent fracture behaviour of the sheets in a dynamic tension test can be seen, showing a fracture of great ductility.

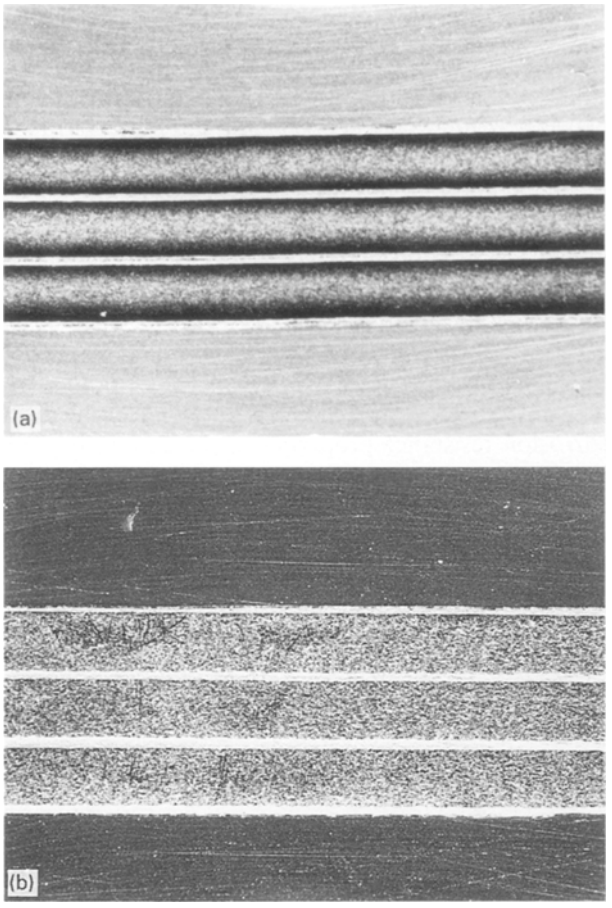

Figure 1 Transverse sections of composite laminates: (a) zinc laminate, (b) Lead–tin laminate, × 20

TABLE I Mechanical properties of reinforced steel sheets

$R_{p0.2}$ (MPa)	R_M (MPa)	A_{80} (%)
175	314	39

2.3. Welding preparation of samples

To be used in peel as well as in tension–shear tests, samples with the dimensions 160 × 40 mm of a three steel sheet composite were prepared. For comparison, pieces of the same dimensions were cut from the as-received 0.5 mm bare steel sheet. These pieces were stacked together in groups of three to have a sample with a similar structure to that of the three multilaminar composite.

The spot welding was made with a SERRA Alfa-13 spot welding machine of 30 kVA power provided with a pressure system of 3000 N maximum. The welding parameters were electronically controlled with a SERRATRON-7000. Water-cooled Cu–Cr–Zr welding electrodes with truncated conical tips were used.

2.4. Welding tests

The peel test was used to determine appropriate welding conditions and to measure the strength of the welds; tension–shear tests were carried out in a tensile machine. An automotive weld quality resistance spot welding recommended practice [11] was followed.

Examples of the peel test and the tension–shear test specimens as-welded conditions are shown in Fig. 3a and b, respectively. Fig. 4 shows the results of a peel

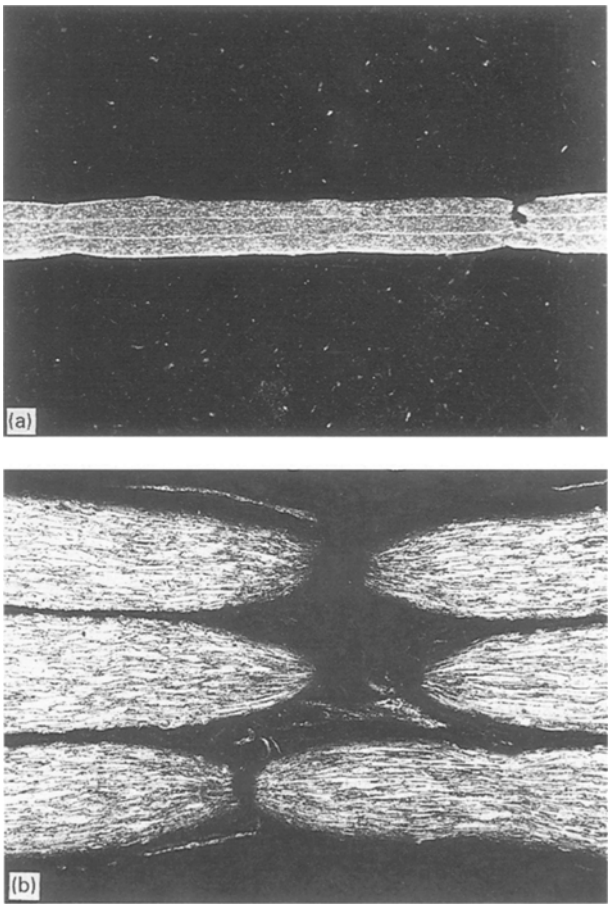

Figure 2 Typical aspect of fracture of laminates in a dynamic tension test.

test applied to a specimen similar to that of Fig. 3. As quality criteria, the appearance and size of the weld buttons were used. Optical and scanning electron microscopy were used to study the microstructure before and after welding as well as the element distribution.The interlayer thickness was measured in an optical microscope using an appropriate ocular and the weld diameters were measured from micrographs with magnification of $\times 7$.

2.5. Welding procedure

Given the different natures of the multilaminar composites, the welding process was adjusted bearing in mind the physical properties of the interlayer materials and reinforced steel. In Table II, the physical properties of pure zinc, lead, tin and iron are shown. Two welding processes for the multilaminar composites and a third one, for comparison, for the steel sheets, were established.

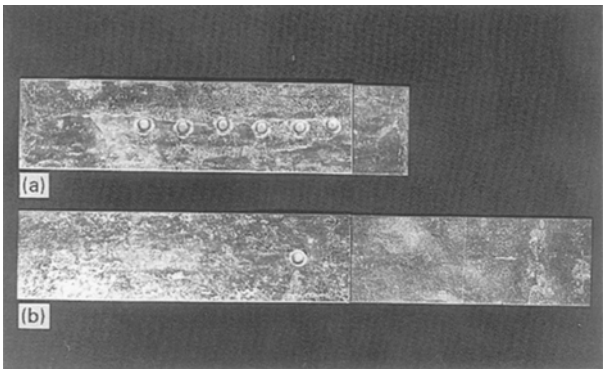

Figure 3 Weld test specimens. (a) peel test; (b) tension shear test.

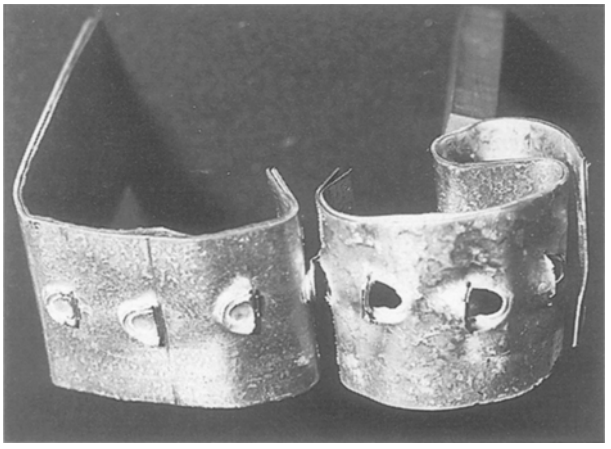

Figure 4 Aspect of the peel test specimen showing acceptable behaviour.

2.5.1. Weld parameters

For the structure with the Pb–Sn interlayers, two different welding conditions, I and II in Table III, were found to produce satisfactory results. It was intended that both conditions represented a similar weld input energy. For the structure with the Zn–Zn/Fe interlayers, only condition II was successful. Attempts to use condition I resulted in weld spattering. The parameters needed to weld the bare stacked sheets correspond to condition III. It is apparent that a lower weld energy is needed for the as-received steel sheets.

3. Discussion

3.1. Resolidification of the non-ferrous interlayers

On welding under condition I the zinc multilaminar composite spatters, probably due to the high weld current and the relatively short welding time (13 cycles) that produce a high rate of energy input. Under this condition the zinc is vaporized due to its low boiling temperature.

Initially the molten zinc is resolidified, forming an external ring around the weld spot that works as a hermetic seal. As the temperature in the spot zone increases, the seal breaks because of the high pressure produced as a consequence of the vaporization of zinc, splashing out the still liquid zinc inside.

Fig. 5a and b show the ruptures in the tension–shear test of two spot welds in zinc and lead–tin laminates, respectively. The central circle corresponds to the shear failure section of the weld, and the first ring, covering the area under the electrode tips, is a zone without interlayer free material. The interlayer has been squeezed out radially from between the facing interfaces of the joint and placed around the first ring, developing the second one. Some radial splashes may be seen on the external side of the external ring (Fig. 5a).

It can be observed that the second ring of the zinc multilaminar composite is more continuous and compact than that of the lead–tin composite, making a better seal, which facilitates the build up of vapour pressure and zinc spattering. The lead–tin multilaminar composite has less probability to develop a continuous ring because of the lower melting temperature and the thermal conductivity of the constituent lead and tin elements as well as their higher electrical resistivity; all these factors contribute to keep the matrix material in a liquid state.

Satisfactory results were obtained, however, under condition II for the zinc multilaminar composite. The lower welding current (lower energy input rate) fa-

TABLE II Physical properties of materials used in multilaminar composites

Material	Melting point		Boiling point		Thermal conductivity		Resistivity
	(K)	(°C)	(K)	(°C)	($W m^{-1} K^{-1}$)	($cal h^{-1} m^{-1} °C^{-1}$)	($10^{-2} \Omega m$)
Fe	1809	1536	3273	3000	82	14	9.7
Zn	692	419	1180	907	120	—	5.9
Pb	600	327	2023	1750	35	—	20.6
Sn	504	231	2543	2270	60	—	11

TABLE III Welding parameters

Condition	Weld current (kA)	Welding time (cycles)	Load (N)
I	8.7	13	2000
II	7.7	20	1750
III	6.5	12	2250

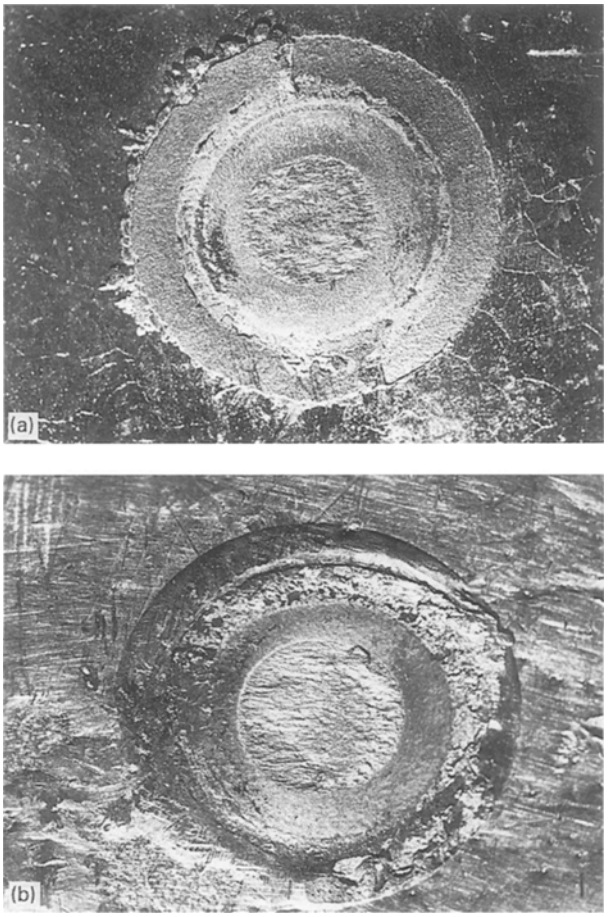

Figure 5 Samples showing various zones of shear failure sections: (a) zinc laminate, (b) lead–tin laminate, × 7.

voured the squeezing out of zinc from between the electrodes before its boiling point was reached, giving less zinc vapour and avoiding spatters. However, under this condition it was necessary to increase the welding time and to lower the electrode load relative to condition I, in order to achieve acceptable spot-weld diameters.

Lead–tin multilaminar composites show good weldability in both conditions I and II. The low melting and the high boiling points, together with the favourable electrical resistivity and thermal conductivity of lead and tin to generate and keep the welding heat concentrated, lead to good welding results for this multilaminar composite.

Condition III, used for welding the stacked bare steel sheets, provided about one-half of the input energy of conditions I or II, which was enough to obtain acceptable welds in this material. A higher electrode load was required to adjust the initial contact electrical resistances.

3.2. Characteristics of the welds

The general appearances of welds (Fig. 3), are similar in both types of multilaminar composites, presenting in all cases electrode indentations on the external surfaces. Fig. 6a and b show two weld cross-sections of only one of the three laminar composites of zinc and lead–tin, respectively. In both cases a collapsing effect of the surfaces under the pressure of the electrodes can be seen; this corresponds to the thickness of the non-ferrous interlayers between the reinforcing steel sheets.

The initial electrical heating developed from the initial contact resistance, melts the interlayer between the steel sheets because of the low melting points of the constituent metals, and originates the general heating of the zone under the electrodes. As a consequence, under the electrode pressure the surface collapses, causing the electrode indentations and, at the same time, squeezing out the melted non-ferrous metal from the zone between the electrodes.

The squeezed materials remain displaced at the periphery of this zone between the internal sheets of the composite, producing a thickening nearby, as can be seen in Fig. 6. This thickening is larger in the closest interlayer to the weld buttton. Between the two three-laminar composites a ring is produced, as described in Section 3.1 above, between the facing surfaces of the joint.

Traces of the interlayer can be optically detected between the reinforcing sheets at the weld zone of both

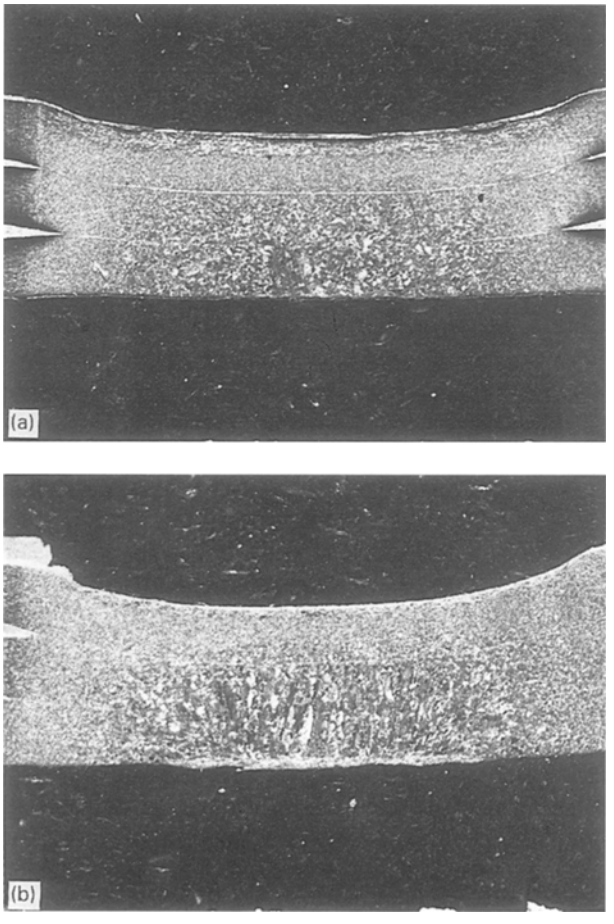

Figure 6 Transverse section of spot welds in (a) zinc laminate, and (b) lead–tin laminate × 20.

types of composite, being clearly visible as thin lines in the same photographs, especially in the zinc laminate (Fig. 7a). Because the low-melting non-ferrous interlayer material has been expelled, these thin layers must correspond to a higher melting point Fe–Zn alloyed layer in the zinc composite and, due to the immiscibility of lead in iron, to a much thinner Fe–Sn alloyed layer in the lead–tin laminate.

After the interlayer has been expelled, electrical resistances for the welding heat generation are created from the contacts between the preceding layers. Thus, in zinc multilaminar composites, owing to the low electrical resistivity and high thermal conductivity of this element, less heat is developed, and a finer granular microstructure is obtained than in lead–tin multilaminar composites. This can also be observed in previous photographs (Fig. 6) in addition to the greater depth of the melted zone at the lead–tin multilaminar composite. Fig. 7a and b, show a higher magnification view of these microstructures in two welded spots of both multilaminar composites.

In the zinc multilaminar composites, the possibility for zinc to diffuse into the steel also exists. X-ray analysis by scanning electron microscopy was used to determine the amount of zinc in the welded zone. Only iron was found (Fig. 8) and, as can be seen in mapping of Fig. 9, no significant trace of zinc was found in the weld.

The spot welds made in stacked bare sheets are very similar to those of the lead–tin multilaminar composites in regard to the grain size, showing a wide melted zone that spreads over the whole thickness of the three reinforcing sheets. The higher contact resistances at the iron–iron interfaces, and the relatively high electrical resistivity of this metal, caused the heat developed to be similar to that of the lead–tin multilaminar composites.

In both the zinc and lead–tin multilaminar composites and the bare sheet packets, the diameter of the melted zone in such a single sheet decrease from the weld centre to the electrodes. This gives a typical stepped appearance, common to the three types of structure, to the weld buttons resulting from the peel test, as is illustrated in Fig. 10.

3.3. Influence of the interlayer thickness on the strength

In Table IV the results from the tension–shear tests are presented. The failure mechanisms marked A and B correspond to the failure appearance shown in Fig. 11a and b, respectively, coming from fractured samples of that test. In the specimens failing by

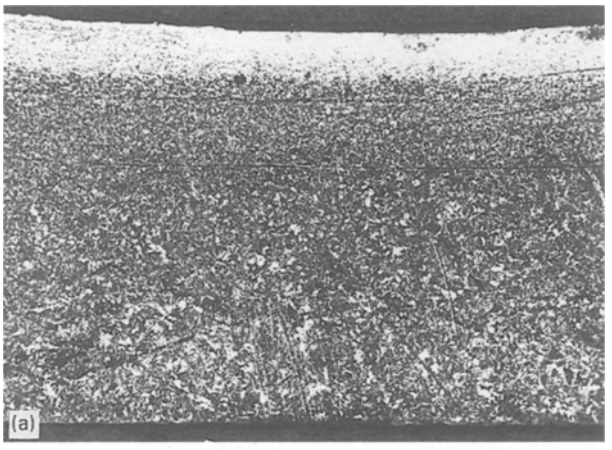

Figure 7 Microstructure of the weld region: (a) zinc laminate, and (b) lead–tin laminate, × 50.

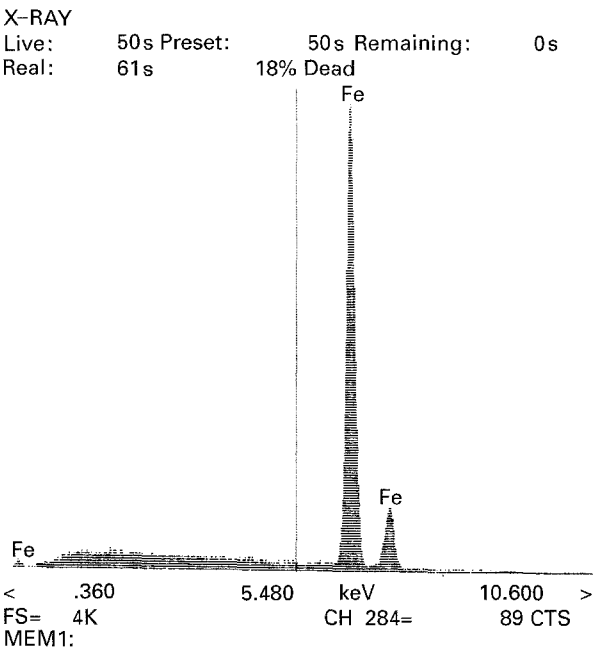

Figure 8 X-ray analysis of the zinc laminate.

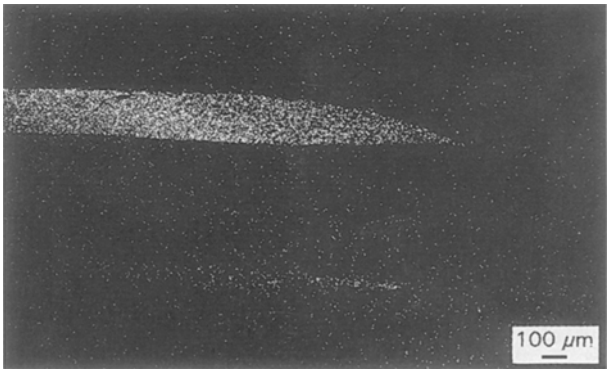

Figure 9 X-ray mapping of zinc near a weld nugget.

mechanism A, the composites were separated by pure shear of the weld nugget. The failure section is the central circle of fibrous aspect of these samples. The specimens failing by mechanism B show a button of weld material torn out from one of the multilaminar composites of the welded joint.

It can be observed that this last mechanism was produced in the lead–tin multilaminar composites at the highest failure loads in both weld conditions I and II. However, this mechanism never occurred in the zinc multilaminar composites, in spite of fracturing in some cases even at higher loads than the lead–tin multilaminar composites. This could be because of the better metallurgical quality of the weld spots of zinc multilaminar composites, due to its finer grain size.

It can also be observed that these cases of higher weld strengths correspond to lower thickness of matrix material. In Fig. 12 the failure loads are plotted as a function of the total matrix thickness between the steel reinforcing sheets. The alignment of data confirms this general trend: smaller interlayer thicknesses resulting in higher mechanical strengths, regardless of which matrix material was used.

On the other hand, the load capacity of the weld spots is very high, considering the size of the fibrous failure sections of the spots, whose diameters ranged between 3.8 and 5 mm. In general, the resulting tensile strengths of the lead–tin multilaminar composites are over 500 MPa, and even over 600 MPa for the zinc multilaminar composites. A possible explanation of these extremely high loads could be the appearance of some kind of brazing or soldering weld around the melted nugget of the spots.

This kind of bonding appears in most of the areas of the first ring (Fig. 5) between the Fe–Zn or Fe–Sn alloyed layers of both types of multilaminar

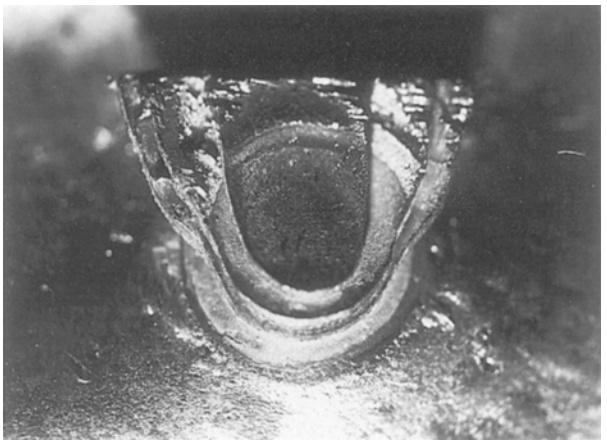

Figure 10 Typical stepped weld button from a peel test specimen.

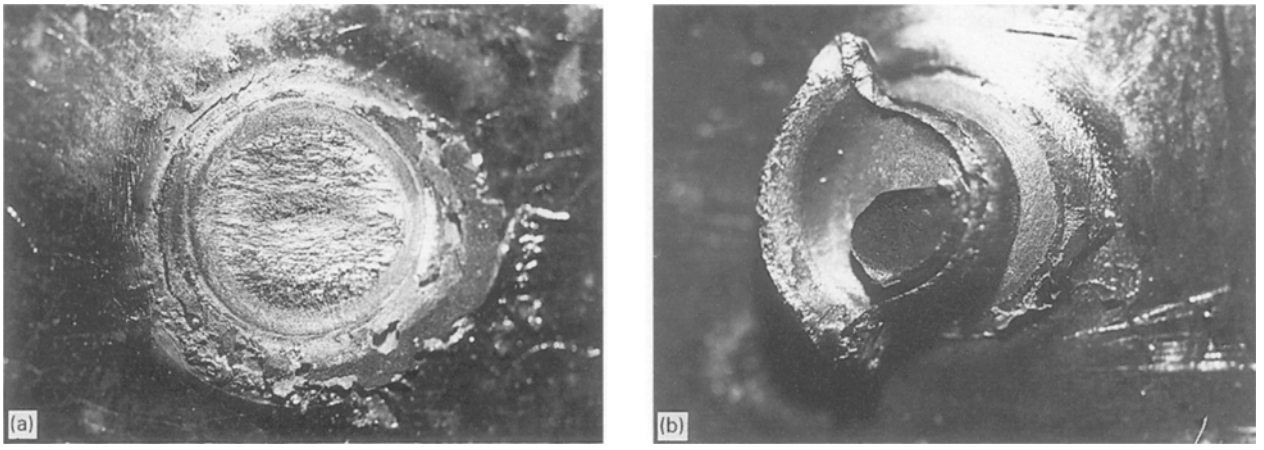

Figure 11 Failure mechanism according to Table IV; (a) mechanism A, and (b) mechanism B.

TABLE IV Type of fracture and tensile test data

Interlayer	Welding condition	Failure mechanism	Average interlayer thickness (μm)[a]	Weld diameter (mm)	Failure load (N)
Pb–Sn	I	A	172	3.8	7250
Pb–Sn	I	A	85	4.1	7150
Pb–Sn	I	B	82	5.1	9360
Pb–Sn	II	A	142	—	4800
Pb–Sn	II	A	101	4.5	8530
Pb–Sn	II	B	46	5.0	10010
Zn	II	A	118	3.8	7640
Zn	II	A	88	3.8	8040
Zn	II	A	94	3.8	8430
Zn	II	A	86	4.0	8820
Zn	II	A	65	4.7	10190
Zn	II	A	62	4.9	10680
None	III	B	—	5.9	8360

[a]Defined as the average of the four inside interlayers in two three-layer specimens.

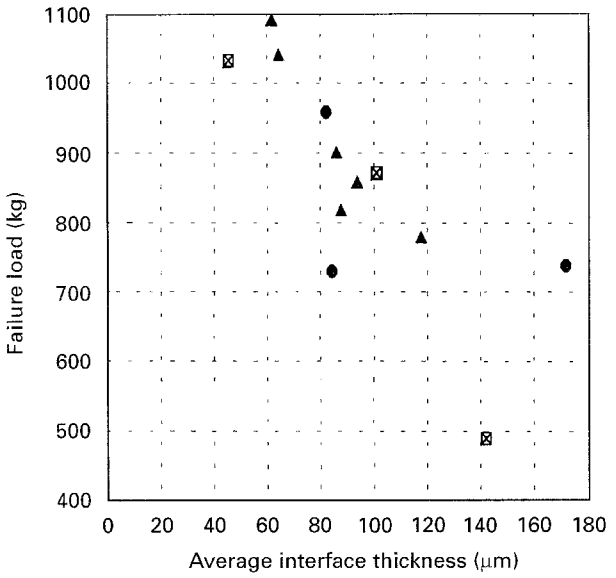

Figure 12 Failure loads versus total interlayer thickness. (●) Sn–Pb interfaces, condition I; (⊠) Sn–Pb interfaces, condition II; (▲) Zn interfaces.

composites. Taking this area also to be part of the failure section in addition to the central fibrous area, the calculated tension strength would be about 300 MPa, similar to the strengths of the steel base material.

4. Conclusions

The spot weld characteristics of a steel multilaminar composite of low-carbon steel reinforcing sheets with zinc or lead–tin matrix interlayers were investigated. The following conclusions can be made.

1. Both multilaminar composite materials show good weldability features for the resistance spot-weld process. The structure containing a zinc interlayer was found somewhat more difficult to weld, because of the low electrical resistivity and the high thermal conductivity of the zinc interlayer. The formation of a sealing ring of zinc around the weld zone causes this multilaminar composite to have a greater tendency to produce spatters.

2. The external weld appearance was independent of the composition of the interlayer material, both showing significant indentations from the electrode tips.

3. The zinc interlayer multilaminar composite was found to have a lower heat-affected volume and finer grain size than the lead–tin interlayer multilaminar composite. Thin layers of intermetallic Fe–Zn or Fe–Sn remain between the steel reinforcing sheets next to the squeezed out material from the weld zone under the electrode pressures.

4. The interlayer thickness significantly influences the mechanical strength of the points. Decreasing the thickness improves the mechanical properties regardless of the interlayer composition.

5. The weld spots in the zinc interlayer multilaminar composites showed greater strength and the failure mechanism at the tension–shear test was shear rupture. In the lead–tin interlayer multilaminar composites, the welds of higher strength ruptured by the weld-button mechanism. This failure behaviour is likely to have been determined by the better quality of the zinc interlayer multilaminar composite welds, due to their finer metallurgical structure.

6. The shear failure loads were extremely high in relation to the weld-spot diameters. It is supposed that an additional zone around the fibrous sheared section of the welds could have contributed to these high strengths by the formation of some kind of brazing or soldering welds between the layers on intermetallics Fe–Zn or Fe–Sn, depending on the interlayer composite type, remaining at the weld zones.

A better evaluation of the above conclusions requires additional research into the best conditions for the weldability of these multilaminar composites and will provide a more complete knowledge of the spots formation, kinds of weld involved, quantification of the influence of the interlayer thickness and possible contributions of all factors involved to the final strengths of the weld spots.

Acknowledgements

The authors thank the European Community for the grant received by Eng. Haakan Engstrom, Human Capital and Mobility Program, for the stay at CENIM during 1994. This work is an additional contribution to the previous work of the Project "Development of New Composite Materials of Steel and Zinc Matrix" 7210-MB/931-90F4.02A, made with funds from EU (1991–1994).

References

1. J. D. EMBURY, N. J. PETCH, A. E. WRAITH and E. S. WRIGHT, *Trans. TMS AIME* **239** (1967) 149.
2. T. P. STUART and I. G. CROUCH, *Int. J. Adhes.*, **12** (1992) 3.
3. H. W. KUM, T. QYAMAL, J. WADSWORTH and O. SHERBY, *J. Mech. Phys. Solids* **31** (1983) 173.
4. B.C.SNYDER, J. WADSWORTH and O. SHERBY, *Acta Metall.* **32** (1984) 919.
5. S. LEE, J. WADSWORTH and O. SHERBY, *J. Compos. Mater.* **25** (1991) 842.
6. Y. OHASHI, J. WOLFENSTINE, R. KOCK and O. SHERBY, *Mater. Sci. Eng.* **A151** (1992) 37.
7. A.J. VÁZQUEZ-VAAMONDE and J. J. DE DAMBORENEA, *Proc. Adv. Mater.* **1** (1991) 55.
8. *Idem., Mater. Des.* **14** (1993) 197.
9. A.J. VÁZQUEZ-VAAMONDE, *J. Phys.* **IV** Supl. 3 (1992) 773.
10. *Idem*, Final Report ESCC 7210-MB/931-90-F4.02A, 1991–1993, Development of New Multilayer Materials of Steel and Non-ferrous Matrix, D.G. XII, Brussels.
11. Recommended Practice for Automotive Weld Quality-Resistance Spot Welding, ANSI/AWS D8.7–88 (American Welding Society, Miami, 1988).

Received 15 September
and accepted 25 October 1995